

WALTERS LIQUID B NANOFLUID FLOW INDUCED DUE TO A MICRO POLAR EFFECT UNDER CASSON PARAMETER

P.S.S.NAGALAKSHMI¹ AND N. VIJAYA

ABSTRACT. In the present investigation is to Walters liquid B nanofluid flow induced due to a micro polar effect under Casson parameter with carbon nanotubes. The boundary layer flow and heat transfer to a Walters liquid B nanofluid with casson effect model over a stretching surface is introduced. The Walters liquid B nanofluid model is used to characterize the behavior of the fluids having transition parameter (Ts) with adequate micropolar effect to obtained the nature of Casson and non Casson effect with different basefluid. The modeled boundary layer conservation equations are converted to non-linear coupled ordinary differential equations by a suitable transformation. Python language with bvp solver was adopted to obtained numerical solutions of the resulting equations by using the Runge-Kutta method along with shooting technique. This analysis reveals many important physical aspects of flow and heat transfer. Computations are performed for different values of the radiation parameter (Tr), the elastic deformation parameter (δe) and the elastic parameter (ϵ_1). A comparison with previously published data in limiting cases is performed and they are in excellent agreement.

1. INTRODUCTION

The theory of microfluids introduced in [1] deals with a class of fluids which exhibit certain microscopic effects arising from the local structure and micro-motions of the fluid elements these fluids can support stress movements and

¹corresponding author

2010 *Mathematics Subject Classification.* 80A99, 35Q79, 74F10.

Key words and phrases. Transition component, Python, CNT.

body movements and are influenced by the spin inertia. A sub-class of these fluids is the micro polar fluids which exhibits the micro rotational effects and micro rotational inertia. The micropolar fluids can support couple stress and body couples only. Physically they may represent adequately the fluids consisting of bar like elements. This theory has presented an excellent model to examine many complex fluids some of them are liquid crystals, the flow of low concentration suspension, blood and turbulent shear flows also body fluids and biological flow problems have been modelled by micropolar theory.

The boundary layer theory was presented by Ludwig Prandtl. The main idea was to divide the flow into two parts. The smaller part is a thin layer in the vicinity of solid surface in which the effects of viscosity are felt. This thin layer near the solid surface is called boundary layer. The larger part concerns a free stream of fluids, far from solid surface which is considered to be non-viscous. Although the boundary layer is thin, it plays an essential role in fluid dynamics. The boundary layer theory is used very frequently for solving fluid flow and heat transfer problems.

Radiation is a transfer of thermal energy in the form of electromagnetic waves. Like electromagnetic radiation(light, X-ray, microwaves)thermal radiation travels at the speed of light passing most easily through vacuum or nearly transparent gases. Both conduction and convection require matter to transfer heat. Radiation is a method of heat transfer that does not rely upon any contact between heat source and the heat object. Radiative heat transfer is of utmost importance in high temperature applications such as combustion of fossil fuels, operation of a Furness, thermal cracking and the tube stills in petroleum refineries etc.

The flow and heat transfer characteristics of free convection micropolar fluid theory and simulation of micropolar fluid dynamics are described in [2]. Micropolar fluid behavior on steady MHD free convection and mass transfer flow with constant heat and mass fluxes, joule heating and viscous dissipation was investigated in [3]. Periodic magnetohydrodynamic natural convection flow of a micropolar fluid with radiation was examined in [4]. Time-dependent natural convection of micropolar fluid in a way triangular cavity was reported in [5]. On stagnation point flow of a micropolar nano fluid past a circular cylinder with velocity and thermal slip was extended in [6]. Study of the couple stress convective micropolar fluid flow in a hall MHD generator system was presented in [7]. Numerical analysis of water based CNT's flow of micropolar

fluid through rotating frame was investigated in [9]. Magnetic fluid influence in three-dimensional rotating micropolar nano liquid with convective conditions was analysed in [10]. Numerical investigation on transport of momenta and energy in micropolar fluid suspended with dusty, mono and hybrid nano structures was studied in [11].

The problem of Walter's Liquid B nanofluid flow over a stretching sheet with an inclined magnetic field due to the effect of micropolar rotation under casson parameter with adequate boundary conditions are solved computationally with Python coding.

2. MATHEMATICAL FORMULATION

Formulation of the problem is under the assumption that the nano fluid is incompressible, Non-Newtonian (mixed fluid, electrically conducting and magnetically susceptible, permeable stretching surface which coincide with the sheet $z=0$, the flow being in the region $z > 0$. The physical variables in this model in the cartesian co-ordinate system are functions of y and z respectively. It is assumed that the sheet wall temperature is sufficiently high to affect radiative heat transfer. So, if the axial velocity p , velocity of the fluid q and it is a velocity at which the fluid is sucked by the wall, also in comparisons with applied inclined magnetic field induced magnetic field is neglected so that $B = (0, 0, B_0)$ parallel to z -axis and electric field. $E = (-E_0, 0, 0)$ parallel to x -axis with slip velocity.

To start with basic governing equations for this investigation is based on the balances of mass, linear momentum and energy are as follows [8].

$$(2.1) \quad \frac{\partial p}{\partial y} + \frac{\partial q}{\partial z} = 0,$$

$$(2.2) \quad \begin{aligned} p \frac{\partial p}{\partial y} + q \frac{\partial p}{\partial z} = & \left[\frac{T_s}{2} - \left(1 - \frac{1}{\epsilon} \right) \nu_{nf} + \frac{k_e}{\rho_{nf}} \right] \frac{\partial^2 p}{\partial z^2} \\ & - \epsilon_0 \left[p \frac{\partial^3 p}{\partial y \partial z^2} + q \frac{\partial^3 p}{\partial z^3} + \frac{\partial p}{\partial y} \frac{\partial^2 p}{\partial z^2} - \frac{\partial p}{\partial z} \frac{\partial^2 p}{\partial y \partial z} \right] \\ & - \frac{\sigma_{nf} B_0^2}{\rho_{nf}} p \sin^2 \gamma_1 - g \frac{(\rho \beta)_{nf}}{\rho_{nf}} (T - T_i) \cos \gamma_2 \\ & + \frac{\sigma_{nf}}{\rho_{nf}} E_0 B_0 \sin \gamma_1, \end{aligned}$$

$$\begin{aligned}
 (2.3) \quad p \frac{\partial T}{\partial y} + q \frac{\partial T}{\partial z} &= \frac{k_{nf}}{(\rho c_p)_{nf}} \frac{\partial^2 T}{\partial z^2} - \frac{1}{(\rho c_p)_{nf}} \frac{\partial q_r}{\partial z} \\
 &\quad - \frac{\delta e \epsilon_0}{c_p} \left[\frac{\partial p}{\partial z} \frac{\partial}{\partial z} \left[p \frac{\partial p}{\partial y} + q \frac{\partial p}{\partial z} \right] \right] \\
 &\quad + \frac{\mu_{nf}}{(\rho c_p)_{nf}} \left(\frac{\partial p}{\partial z} \right)^2 + \frac{Q^*}{(\rho c_p)_{nf}} (T - T_i) \\
 &\quad - \frac{\sigma_{nf}}{(\rho c_p)_{nf}} (p B_0 \sin \gamma_1 - E_0)^2,
 \end{aligned}$$

$$(2.4) \quad p \frac{\partial \Omega}{\partial y} + q \frac{\partial \Omega}{\partial z} = \frac{G^*}{\rho_{nf} j} \frac{\partial^2 \Omega}{\partial z^2} - \frac{k_e}{\rho_{nf} j} \left[\frac{\partial p}{\partial z} + 2\Omega \right].$$

With boundary conditions

$$\begin{aligned}
 p &= cy + r^* \left[(\mu + k_e) \frac{\partial p}{\partial z} + k_e \Omega \right] \\
 q &= q_w \\
 \frac{\partial T}{\partial z} &= -(j)^{-0.5} S \left(\frac{y}{l} \right)^2 \quad \text{as } z \rightarrow 0 \\
 l &= \left(\frac{\nu}{c} \right)^{0.5} \\
 \Omega &= -n \frac{\partial p}{\partial z} \\
 T &= T_w = T_i + S \left(\frac{y}{l} \right)^2 \\
 p &\rightarrow 0, \Omega \rightarrow 0, T \rightarrow T_i \quad \text{as } z \rightarrow \infty,
 \end{aligned}$$

where p and q are velocity components of y and z axes respectively. Ω denotes micro rotation component, T_s is the transition state parameter, ϵ Casson parameter, k_e erigen vortex viscosity, ϵ_0 elastic parameter, β thermal expansion coefficient, k_{nf} thermal conductivity of nano fluid, σ_{nf} electrical conductivity of nano fluid, δ_e elastic deformation parameter, G^* gyroscopic viscosity, S is the thermal property of the liquid, l is a characteristic length, and j is micro inertia per unit mass. When $n = 0$, microelements close to the wall are not able to rotate, when $n = 0.5$, this indicates weak concentration of micro-elements as elaborated. When $n = 1.0$, specifies turbulent boundary layer flows. Here the threshold value of n ranges from 3 to 10, because of nanofluid having blood

as base fluid along with CNT, but the threshold value of n ranges from 1 to 10, when the base fluid is water, kerosine oil and engine oil along with CNT.

2.1. Similarity Transformations.

$$\begin{aligned}
 p &= cyf^1(\eta) \\
 q &= -(cy)^{0.5}f(\eta) \\
 \eta &= \left(\frac{c}{\nu}\right)^{0.5}z \\
 \theta(\eta) &= \frac{T - T_i}{T_w - T_i} \\
 \Omega(\eta) &= cy\left(\frac{c}{\nu}\right)^{0.5}g(\eta).
 \end{aligned}
 \tag{2.5}$$

The above transformations satisfy equation (2.1) automatically, and equations (2.2)–(2.4) with equation (2.5) reduce to the following ODEs:

$$\begin{aligned}
 &\epsilon_1 [2f^1 f^{111} - f f^{IV} - (f^{11})^2] \\
 &= -[(f^1)^2 - f f^{11}] \\
 &+ \left[\frac{H_1}{H_2} \left[\frac{Ts}{2} - \left(1 - \frac{1}{\epsilon}\right) \right] + \frac{Ke}{H_2} \right] f^{111} \\
 &- \frac{M2H_3}{H_2} f^1 \sin^2 \gamma_1 - \frac{H_4}{H_2} (Gry) \theta \cos \gamma_2 \\
 &+ \frac{Ke}{H_2} g^1 + \frac{H_3}{H_2} (E2)(M2) \sin \gamma_1, \\
 \\
 &\theta^{11} \left[1 + \frac{Tr}{H_6} \right] = -\frac{H_5}{H_6} Pr [f\theta^1 - 2\theta f^1] \\
 &- EcPr \left[\frac{H_1}{H_5 H_6} (f^{11})^2 \right] \\
 &+ \frac{H_5}{H_6} \delta e \epsilon_1 EcPr f^1 (f^{11})^2 \\
 &- \delta e \epsilon_1 \frac{H_5}{H_6} EcPr f f^{11} f^{111} \\
 &- \frac{H_5}{H_6} EcPr (M2) [f^1 - (E2)]^2 \\
 &- \frac{QPr}{H_6} \theta,
 \end{aligned}$$

$$g^{11} \left[1 + \frac{Ke}{2} \right] = Ke[f^{11} + 2g] - H_2[f^1 g - f g^1].$$

2.2. Boundary Conditions.

$$\begin{aligned} f(\eta) &= S_1, \quad f^1(\eta) = 1 + \alpha[(1 + Ke)f^{11}(\eta)] \\ g(\eta) &= -nf^{11}(\eta) \quad \theta^1(\eta) = -1 \quad \text{as} \quad \eta \rightarrow 0 \\ f^1(\eta) &\rightarrow 0, \quad g(\eta) \rightarrow 0, \quad \theta(\eta) \rightarrow 0 \quad \text{as} \quad \eta \rightarrow \infty, \end{aligned}$$

where

$$\begin{aligned} Ke &= \frac{k_e}{\mu_f}, \quad \alpha = r^* \left(\frac{c}{\nu_f} \right)^{0.5} \mu_f, \quad \epsilon_1 = \frac{\epsilon_0 c}{\nu_f}, \quad M_2 = \frac{\sigma_f B_0^2}{c \rho_f}, \quad E2 = \frac{E_0}{B_0 P_\omega}, \\ Gry &= \frac{g \beta_f \Delta T \frac{y^3}{\nu_f^2}}{\frac{p_w y^2}{\nu_f^2}}, \quad Pr = \frac{\mu_f c_p}{k_f}, \quad Ec = \frac{c^2 l^2}{S c_p}, \quad Tr = \frac{16 \sigma^s T_i^3}{3 k^s k_f}, \quad j = \frac{\nu_f}{c} \\ H_1 &= \frac{1}{(1 - \phi)^{2.5}}, \quad H_2 = (1 - \phi) + \phi \frac{\rho_C N T}{\rho_f} \\ H_3 &= 1 + 3 \frac{(\sigma_{CNT} - \sigma_f) \phi}{[\sigma_{CNT} + 2\sigma_f] - [\sigma_{CNT} - \sigma_f]}, \quad H_4 = \left[(1 - \phi) + \frac{(\rho \beta)_{CNT}}{(\rho \beta)_f} \phi \right] \\ H_5 &= (1 - \phi) + \phi \frac{(\rho c_p)_{CNT}}{(\rho c_p)_f}, \quad H_6 = \frac{(1 - \phi) + 2\phi \frac{k_{CNT}}{k_{CNT} - k_f} \ln \left(\frac{k_{CNT} + k_f}{2k_f} \right)}{(1 - \phi) + 2\phi \frac{k_f}{k_{CNT} - k_f} \ln \left(\frac{k_{CNT} + k_f}{2k_f} \right)}. \end{aligned}$$

2.3. Engineering Parameters.

$$\begin{aligned} cf_y &= \frac{2\tau_\omega}{\rho_{nf}(cy)^2}, \quad \tau_\omega = \left[(\mu_{nf} + k_e) \frac{\partial p}{\partial z} + k_e \Omega \right]_{z=0} \\ (Re_y)^{(0.5)} cf_y &= 2[H_5 + (1 - n)Ke]f^{11}(0), \quad cw_y = \frac{m_\omega j}{\rho c \nu y^3} \\ m_\omega &= G^* \left(\frac{\partial \Omega}{\partial z} \right)_{z=0}, \quad cw_y Re_y = \left(1 + \frac{Ke}{2} \right) g^1(0) \\ Nu_y &= \frac{y q_w}{k(T_w - T_i)}, \quad (Re_y)^{(-0.5)} Nu_y = -\theta^1(0)H_6. \end{aligned}$$

TABLE 1. Nature of the nanofuid with transition parameter

Transition values	Nature of fluid	Base fluid	Nanoparticles
$Ts=2$, $\epsilon=1$, $Ke=0$	Walter's liquid B fluid under non casson state	Water,Kerosen oil,Engine oil	SWCNT,MWCNT
$Ts=2$, $\epsilon=1$, $Ke>0$	Walter's liquid B fluid with micropolar effect under non casson state	Water,Kerosen oil,Engine oil	SWCNT,MWCNT
$Ts=4$, $\epsilon>1$, $Ke>0$	Walter's liquid B fluid with micropolar effect under casson state	Water,Kerosen oil,Engine oil	SWCNT,MWCNT
$Ts=4$, $\epsilon>1$, $Ke>0$	Walter's liquid B fluid with micropolar effect under casson state	blood	SWCNT,MWCNT

3. RESULTS AND DISCUSSION

The framework of this study is to scrutinize the properties of SWCNT and MWCNT on Walter's liquid B nanofuid with micropolar effect under casson state parameter over a variable thickness of stretched sheet. Python with bvp scheme has been executed to elucidate the present ODEs. The inducement of SWCNT and MWCNT on velocity, temperature and concentration is portrayed and discussed. Investigators introduced $1 \leq M_2 \leq 5$, $0.01 \leq E_2 \leq 2$, $0.01 \leq Ec \leq 0.2$, $1 \leq \epsilon \leq 5$, $1 \leq Pr \leq 10$, $0.1 \leq \epsilon_1 \leq 1$, $1 \leq Ke \leq 1.8$, $0.01 \leq Gr_y \leq 0.3$, $0.1 \leq Q \leq 0.5$, $0.1 \leq Tr \leq 5$, $3 \leq n \leq 10$, $0.1 \leq \alpha \leq 0.5$, $1 \leq \delta e \leq 5$, $0.01 \leq \phi \leq 0.05$ are the threshold values of the fluid parameters to attain the boundary conditions of the fluid problem through python coding.

3.1. Execution of SWCNT and MWCNT on velocity, thermal and micropolar rotation with blood as a base fluid. Figure 1 to Figure 3 capture the behavior of SWCNT and MWCNT with blood as base fluids on momentum, thermal and

micropolar rotation boundary layers respectively. Influence of momentum, and rotation boundary layers with different base fluids are dominated by MWCNT. Thermal boundary layer is henpecked by SWCNT.

3.2. Execution of SWCNT and MWCNT on velocity, and thermal profile with different base fluid in the absence of Ke . Figure 4 to Figure 5 capture the behavior of SWCNT and MWCNT with different base fluids on momentum, and thermal boundary layers respectively. Momentum boundary layer is subjugated by MWCNT, and thermal boundary layer is conquered by SWCNT.

3.3. Execution of SWCNT and MWCNT on velocity, thermal and micropolar rotation with different base fluid in the presence of Ke . Figure 6 to Figure 8 capture the behavior of SWCNT and MWCNT with different base fluids on momentum, and thermal boundary layers respectively. Thermal and micropolar rotation boundary layers are dominated by SWCNT and momentum boundary layer is occupied by MWCNT.

3.4. Tables of local skin friction coefficient, local Nusselt number and wall coupled stress coefficient. The relative study of present results with those obtained in [8] is shown in Table 1. Behaviour of fluid parameters on local skin friction coefficient, local nusselt number and wall coupled stress coefficient are disclosed in Table 2.

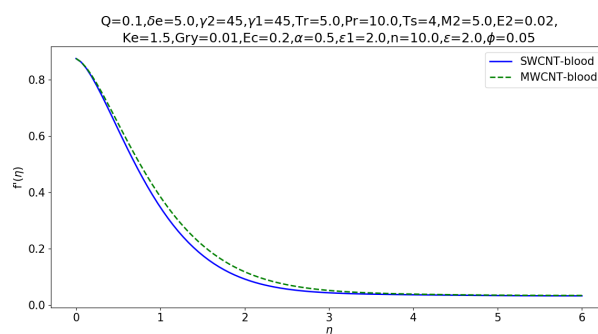


FIGURE 1. Influence of SWCNT and MWCNT on Velocity profile.

TABLE 2. Accuracy assessment for $\theta(0)^1$, when $\gamma_1=90$,
 $Ec=\delta e=E2=Q=\phi=Tr=Ke=Gry=0, Ts=2$

M2	Pr	ϵ_1	[8]	Present
1	1	0.2	1.168700	1.17830

TABLE 3. M2=5, E2=2, Pr=10, Ec=0.2, Q=0.1, Ts=4, n=10,
 $\delta e=5, Tr=5, \gamma_1=45, \gamma_2=45, \phi=0.05, \epsilon=2, \epsilon_1=2$

Ke	$(Re_y)^{0.5} cf_y$		$(Re_y)^{-0.5} Nu_y$		$(Re_y) cw_y$	
	SWCNT	MWCNT	SWCNT	MWCNT	SWCNT	MWCNT
1.1	1.664383	1.7409793	1.77767	1.69467614	-3.27904	-3.17481
1.3	1.999666	2.0917799	1.77767	1.69467614	-3.96902	-3.82913
1.5	2.327063	2.4325610	1.77167	1.68772451	-8.21009	-1.22046
1.7	2.633862	2.7434559	1.75346	1.66438774	-4.45886	-1.87977

TABLE 4. M2=5, E2=2, Pr=10, Ec=0.2, Q=0.1, Ts=4, n=10,
 $Ke=1.5, Tr=5, \gamma_1=45, \gamma_2=45, \phi=0.05, \epsilon=2, \epsilon_1=2$

δe	$(Re_y)^{0.5} cf_y$		$(Re_y)^{-0.5} Nu_y$		$(Re_y) cw_y$	
	SWCNT	MWCNT	SWCNT	MWCNT	SWCNT	MWCNT
1	2.334950	2.4425805	1.7776760	1.6946761	-4.54851	-4.72205
2	2.334950	2.4425805	1.7776760	1.6946761	-4.73077	-4.97864
3	2.334950	2.4418349	1.7776760	1.6941588	-5.09233	-5.43196
4	2.30777	2.4376724	1.7569838	1.6912708	-4.88258	-1.13952

4. CONCLUSIONS

Investigators are concluded that electric field parameter is the major cause of deformations on Walter's liquid B nanofluid under Casson parameter over a variable thickness of stretched sheet with the influence of thermal and micro polar rotation. This investigation has explored that threshold value of micropolar rotation boundary layer is less than the threshold value of thermal and velocity boundary layers because of the effect of erigen vortex viscosity parameter with blood as a base fluid has explored under SWCNT and MWCNT.

It was observed that radiation is the major cause of threshold value of velocity profile diminishes as compared to thermal profile in the absence of erigen vortex

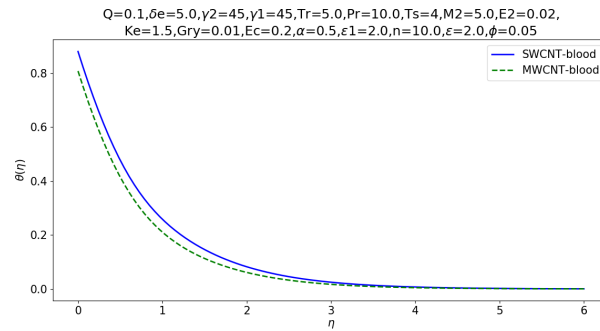


FIGURE 2. Influence of SWCNT and MWCNT on Temperature profile.

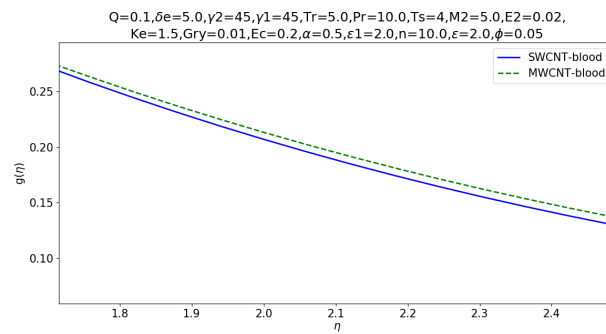
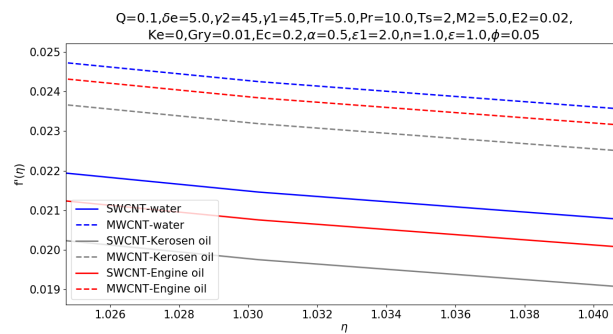


FIGURE 3. Influence of SWCNT and MWCNT on micropolar rotation profile.

FIGURE 4. Influence of SWCNT and MWCNT on Velocity profile with different base fluids in the absence of Ke .

viscosity parameter under the consideration different base fluids with SWCNT and MWCNT.

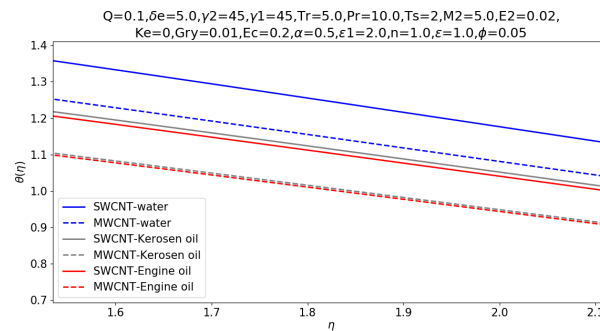


FIGURE 5. Influence of SWCNT and MWCNT on Temperature profile with different base fluids in the absence of Ke .

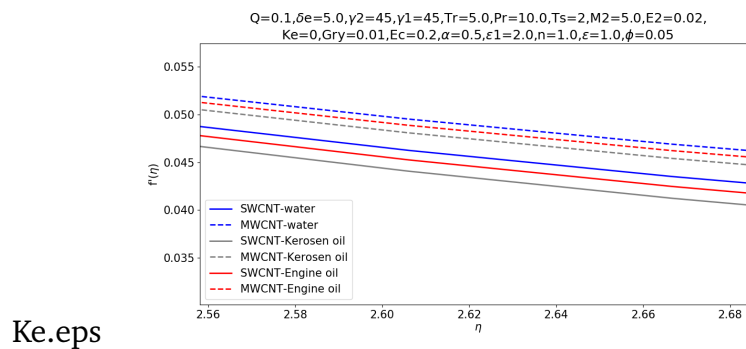


FIGURE 6. Influence of SWCNT and MWCNT on Velocity profile with different base fluids in the presence of Ke .

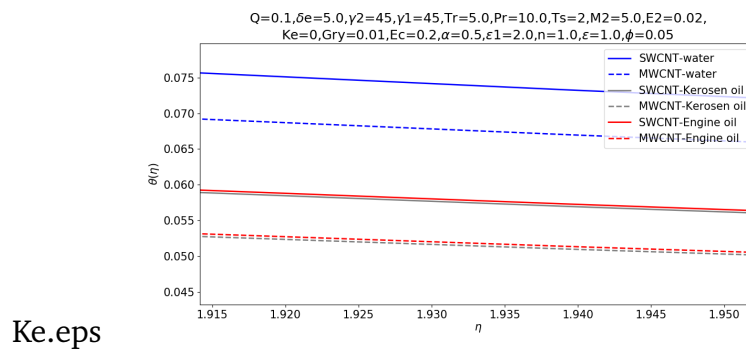


FIGURE 7. Influence of SWCNT and MWCNT on Temperature profile with different base fluids in the presence of Ke .

Investigators noticed that due to electric field parameter, threshold value of velocity profile is enhanced when compared to thermal and micropolar profiles

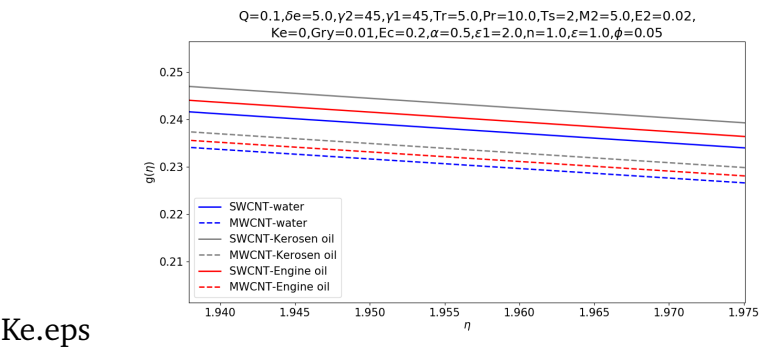


FIGURE 8. Influence of SWCNT and MWCNT on micropolar rotation profile with different base fluids in the presence of Ke .

TABLE 5. $M_2=5, E_2=2, Pr=10, Ec=0.2, Q=0.1, Ts=4, n=10,$
 $Ke=1.5, Tr=5, \gamma_1=45, \gamma_2=45, \phi=0.05, \epsilon=2, \delta e=5$

ϵ_1	$(Re_y)^{0.5} cf_y$		$(Re_y)^{-0.5} Nu_y$		$(Re_y) cw_y$	
	SWCNT	MWCNT	SWCNT	MWCNT	SWCNT	MWCNT
1	2.3209068	2.427889	1.7669844	1.6844837	-3.54846	-3.44533
2	2.3321526	2.436382	1.7755462	1.6903760	-3.62234	-3.49396
3	2.3311904	2.438647	1.7748136	1.6919473	-3.65539	-3.53737
4	2.3326337	2.440157	1.7759125	1.6929949	-3.72015	-3.59959

TABLE 6. $M_2=5, E_2=2, Pr=10, Ec=0.2, Q=0.1, Ts=4, n=10,$
 $Ke=1.5, \gamma_1=45, \gamma_2=45, \phi=0.05, \delta e=5, \epsilon=2, \epsilon_1=2$

Tr	$(Re_y)^{0.5} cf_y$		$(Re_y)^{-0.5} Nu_y$		$(Re_y) cw_y$	
	SWCNT	MWCNT	SWCNT	MWCNT	SWCNT	MWCNT
1	2.2992614	2.41608	1.7505051	1.676292	-3.35620	-3.48037
2	2.3207208	2.42658	1.7668428	1.683581	-3.82231	-6.08175
3	2.3117353	2.42658	1.7600019	1.683581	-2.13320	-3.46959
4	2.3301079	2.43845	1.7739895	1.691816	-2.52934	-7.23590

under the influence of erigen vortex viscosity parameter having different base fluids with SWCNT and MWCNT.

ACKNOWLEDGMENT

Investigators are extremely thankful to Koneru Lakshmaiah Education Foundation and Jawaharlal Nehru Architecture and Fine Arts University for giving a lot of support during this research work at the Department of Mathematics, Koneru Lakshmaiah Education Foundation, Guntur and Department of Digital Technology, Jawaharlal Nehru Architecture and Fine Arts University, Hyderabad.

REFERENCES

- [1] A. C. ERINGEN: *Theory of micropolar fluids*, Journal of Mathematics and Mechanics , **16**(1) (1966), 1–16.
- [2] J. CHEN, C. C. LIANG, J. LEE: *Theory and simulation of micropolar fluid dynamics*, Journal of Nanoengineering and Nanosystems, **224** (2011), 31–39.
- [3] Z. HAQUEA , M. ALAMA , M. FERDOWSBC, A. POSTELNICUD: *Micropolar fluid behaviors on steady MHD free convection and mass transfer flow with constant heat and mass fluxes, joule heating and viscous dissipation*, Journal of King Saud University - Engineering Sciences., **24**(2) (2012), 71–84.
- [4] S. SIDDIQAA, A. FARYADA , N. BEGUMB, M. A. HOSSAINC: *Periodic magnetohydrodynamic natural convection flow of a micropolar fluid with radiation*, International Journal of Thermal Sciences., **111** (2017), 215–222.
- [5] M. A. SHEREMETAB , I. POPC , A. ISHAKD: *Time-dependent natural convection of micropolar fluid in a way triangular cavity*, International Journal of Heat and Mass Transfer., **105** (2017), 610–622.
- [6] N. ABBASA, S. SALEEMBC, S. NADEEMA, A. A. ALDERREMYB, A. U. KHANA: *On stagnation point flow of a micro polar nanofluid past a circular cylinder with velocity and thermal slip*, Results in Physics., **9** (2018), 1224–1232.
- [7] S. ZAHIR, K. POOM, D. ABDULLAH, A. EBRAHEEM, T. PHATIPHAT: *Study of the Couple Stress Convective Micropolar Fluid Flow in a Hall MHD Generator System*, Frontiers in Physics., **7** (2019), 171.
- [8] C. RAGAVAN, S. MUNIRATHINAM, M. GOVINDARAJU, A. K. ABDUL HAKEEM, B. GANGA: *Elastic deformation and inclined magnetic field on entropy generation for walter's liquid B fluid over a stretchning sheet*, Journal of Applied Mathematics and Computational Mechanics., **18**(2) (2019), 85–98.
- [9] S. NADEEMAB, N. ABBASC, Y. ELMASRYD, M. Y. MALIKC: *Numerical analysis of water based CNTs flow of micropolar fluid through rotating frame*, Computer Methods and Programs in Biomedicine., **186**(2) (2020), 105194.

- [10] S. Z. ABBASAB, W. A. KHAN, M. M. GULZAR, T. HAYT, M. WAQAS, Z. ASGHAR: *Magnetic field influence in three-dimensional rotating micropolar nanoliquid with convective conditions*, Computer Methods and Programs in Biomedicine., **189** (2020), 105324.
- [11] H. KANEEZ, J. ALEBRAHEEM, A. ELMOASRY, R. S. SAIF, M. NAWAZ: *Numerical investigation on transport of momenta and energy in micropolar fluid suspended with dusty, mono and hybrid nano-structures*, AIP Advances., **10**(2020), 045120.

DEPARTMENT OF MATHEMATICS
KONERU LAKSHMAIAH EDUCATION FOUNDATION
VADDESWAREM, GUNTUR
ANDHRA PRADESH-522502, INDIA
E-mail address: sathya.krishnat@gmail.com

DEPARTMENT OF MATHEMATICS
KONERU LAKSHMAIAH EDUCATION FOUNDATION
VADDESWAREM, GUNTUR
ANDHRA PRADESH-522502, INDIA
E-mail address: vijayanalleboyina@gmail.com

TABLE 7. Nomenclature

y, z	Cartesian coordinates	p, q	Velocity components of y and z axes
Ω	Micro rotation component	T_s	Transition state parameter
Tr	Radiation parameter	Ec	Eckert number
Pr	Prandtl number	ϵ	Casson parameter
k_e	Erigen vortex viscosity	ϵ_0	Elastic parameter
β	Thermal expansion coefficient	k_{nf}	Thermal conductivity of nanofluid
σ_{nf}	Electrical conductivity of nanofluid	δe	Elastic deformation parameter
G^*	Gyroscopic viscosity	S	Thermal property of the liquid
l	Characteristic length	j	Micro inertia per unit mass
ϕ	Nanoparticle volume fraction	ν_{nf}	Kinematics viscosity of nanofluid
μ_{nf}	Viscosity of nanofluid	μ_{bf}	Viscosity of basefluid
ϕ	Nanoparticle volume fraction	σ_{nf}	Electrical conductivity of nanofluid
σ_{bf}	Electrical conductivity of basefluid	σ_{CNT}	Electrical conductivity of CNT
η	Similarity variable	θ	Dimensionless fluid temperature
g	Dimensionless fluid micropolar rotation	k_{nf}	Thermal conductivity of nanofluid
k_{bf}	Thermal conductivity of basefluid	Gr_y	Grashof number
k_{CNT}	Thermal conductivity of CNT	c_p	Specific heat
T_w	Temperature at the wall	$E2$	Electric parameter
T_i	Temperature of the fluid outside the boundary layer	Ke	Erigen vortex viscosity parameter
$M2$	Magnetic parameter	n	concentration of micro-elements